PHYSICAL REVIEW B VOLUME 15, NUMBER 2 15 JANUARY 1977

Electronic structure of monoclinic selenium (Se_8): Comparison with S_8 and trigonal selenium

W. R. Salaneck, C. B. Duke, A. Paton, and C. Griffiths
Xerox Webster Research Center, Xerox Corporation, Xerox Square-114, Rochester, New York 14644

R. C. Keezer
Xerox Palo Alto Research Center, Palo Alto, California 94304
(Received 12 July 1976)

High-resolution valence electron energy distributions are reported for monoclinic selenium (m-Se, i.e.,Se_8), trigonal selenium, and orthorhombic sulfur (o-S, i.e.,S_8). These data, as well as previously published optical spectra of Se_8 are analyzed using our spectroscopically parametrized CNDO-S (complete neglect of differential overlap, spectroscopically parametrized) molecular-orbital model. The general features of the valence-electron spectra are regarded as direct consequences of the symmetry of the molecular units and the difference in s- and p-electron ionization potentials. Important details in the s-electron photoemission spectra and in the optical-absorption spectra, however, require the full power of the CNDO-S model for their interpretation. We conclude that the photoemission and optical-absorption spectra of m-Se, like those of o-S, can be interpreted directly in terms of the electronic structure of the individual Se_8 and S_8 molecules, respectively.

I. INTRODUCTION

The physical properties of selenium are of interest due to the unique position of selenium at the boundary in column VI between Van der Waals molecular solids (O_2, S_8) and covalent solids (Te). This attribute of selenium is manifested in the variety of allotropic solid-state forms which it can assume. Trigonal (t) Se (and Te) exist as parallel chains, with three atoms per unit cell, arranged in a hexagonal array.[1] Several monoclinic (m) allotropes also occur for Se,[1,2] however, in which the atoms are arranged in eight-membered puckered rings analogous to the structure of S_8 molecules in orthorhombic sulfur,[3,4] but differ somewhat in the packing arrangement of the molecules in the crystal. Although the trigonal form is thermodynamically the most stable,[2] monoclinic crystals can be grown and remain stable for months or longer at room temperature and below. The spectroscopic study of these crystals, with emphasis on establishing their behavior as van der Waals solids,[5,6] is the topic of this paper.

Although extensive electronic-structure calculations[7-12] and spectroscopic studies[7,13,14] of t-Se have been performed, the monoclinic allotropes of selenium have remained relatively neglected.[7] In this paper we report three extensions of earlier studies of α monoclinic selenium (which we shall label as m-Se). First, we present high-resolution x-ray photoemission data which encompass both the Se($4s$)- and Se($4p$)-derived portions of the valence band of m-Se. Second, we show that our CNDO-S (complete neglect of differential overlap, spectroscopically parametrized) molecular-orbital model[6,15-17] provides a satisfactory description both of these data and of previously obtained optical-absorption spectra.[5,7,18] Finally, inspection of the predictions of our CNDO-S molecular-orbital model reveals a rather different interpretation of the photoemission and optical-absorption spectra than those proposed earlier.[5,19,20]

We proceed by presenting a discussion of the experimental details of our study in Sec. II, and details of the CNDO-S model in Sec. III. Section IV contains a discussion of our results and their interpretation. The paper ends with a summary of the important conclusions derived from this study.

II. EXPERIMENTAL PROCEDURES AND SPECTRA

The new measurements reported in this paper are the high-resolution x-ray photoemission valence electron energy distributions for m-Se, t-Se, and orthorhombic sulfur (o-S). Since such electron spectra are thought to be representative of the density of states of the corresponding valence electrons, we adhere to the common practice[6,8-11] of referring to them as "densities of valence states" (DOVS) in spite of the fact that the x-ray induced transition probabilities of s and p electrons are not identical. No spectra of this sort have been reported previously for m-Se, although earlier lower resolution spectra for t-Se,[13] and orthorhombic S,[16] have been published. The present work, however, was carried out using our new fine-focusing, diffraction-type monochromator[21] employing Al($K\alpha$) radiation. The monochromator is fitted to an AEI ES 200B photoelectron spectrometer. The ultimate resolution capabilities are such that the Ag($3d_{5/2}$) line

is recorded with a full width at half maximum of about 0.4 eV. The theoretical width of the monochromatized Al($K\alpha$) radiation, as derived from geometrical considerations, is less than 0.3 eV.[22] The spectrometer has a base pressure of 3×10^{-10} Torr.

The monoclinic selenium single-crystal samples, approximately 0.1 mm thick by several millimeters square in area, were grown from a CS_2 solution at the Xerox Palo Alto Research Center. The surfaces of the samples were initially contaminated with oxygen and carbon. The selenium samples were observed to be self-cleaning after a period of several hours in the vacuum chamber, however, because the vapor pressure of selenium at room temperature is higher than the base pressure of the spectrometer. After this natural sublimation, the Se samples were also found to be free from sulfur contamination.

In addition, polycrystalline samples of m-Se also were prepared by direct precipitation from CS_2. When Se_8 is precipitated out of CS_2 onto gold-foil substrates, a thin adherent polycrystalline film is formed. By crushing the crystallites into the gold with a clean microscope slide cover glass immediately before inserting the samples into the vacuum chamber of the spectrometer, reasonably clean samples could be obtained. For about 50% of the samples no gold signal was observed from the substrate. Most of the crushed crystal samples cleaned themselves of significant carbon and oxygen adsorbed contaminants in a few hours. X-ray diffraction studies, both before and after data acquisition, indicated that these samples were over 90% monoclinic selenium (Se_8).

As a check against sample charging effects, data was collected both in the dark and under illumination of a white microscope light (50 W, focused) in order to exploit the photoconductivity of these materials. No differences in either valence-band (DOVS) or core-level x-ray photoemission spectra (XPS) were observed between the illuminated and nonilluminated samples. In addition, the single-crystal results are essentially identical to those obtained for the crushed crystal except for more noise on the crushed-crystal data.

Single-crystal trigonal selenium [t-Se($10\bar{1}0$)], about 1000 Å in thickness, was grown by vapor-phase epitaxy on ($10\bar{1}0$)-face single-crystal tellurium.[23] The film was deposited at 20 Å/sec onto a cleaved substrate at 120 °C. A small area of the film was detached from the substrate by solution of the tellurium and examined by electron microscopy and diffraction. The trigonal selenium layer was shown to be a good single crystal and contained no grain or subgrain boundaries. The trigonal selenium was only slightly contaminated with carbon and oxygen as received, but it also quickly cleaned itself in the vacuum chamber via sublimation. Orthorhombic sulfur (o-S) samples were prepared, by vapor deposition as previously described.[16] The films of S_8 molecules 50–100 Å in thickness were too thin to support XPS sample charging, as determined by observing the S($2p$) core-level signal during the vapor deposition process. No charging shifts were observed from the lower limit of detectability [i.e., the first observation of the S($2p$) levels at the onset of vapor deposition] up to the end of the experiment.

The XPS valence band data for m-Se are displayed in Fig. 1. The important features to note are the significant depression in the Se(4s)-derived portion of the DOVS at ~ 13 eV binding energy, and the resolution which appears comparable to that afforded by published untraviolet photoemission spectroscopy (UPS) on trigonal selenium.[13] This resolution apparently is controlled by the sample rather than by the spectrometer, once highly monochromatic sources are employed. The nonbonding Se($4p$)-derived portion of the DOVS, from E_F to about 3 eV binding energy, exhibits three features: a main peak with a shoulder on either

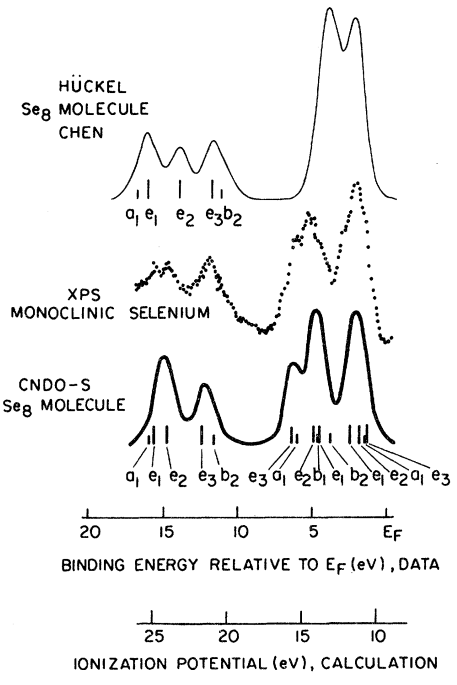

FIG. 1. High-resolution XPS valence-electron photoemission spectra (center panel) for m-Se. These spectra are compared with calculations of the one-electron density of states obtained on the basis of the Hückel model (Ref. 19) (upper curve) and our (CNDO-S) model (lower curve). Each CNDO eigenvalue is represented by a Gaussian of width 0.75 eV in constructing the CNDO-S calculated density of states.

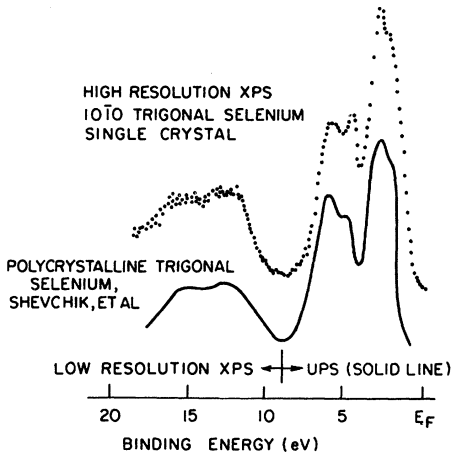

FIG. 2. High-resolution XPS valence-electron photoemission spectrum from t-Se(10$\bar{1}$0) (top panel) compared with an earlier (Ref. 13) composite XPS-UPS spectrum obtained from polycrystalline t-Se.

side, as found for t-Se by UPS.[13] The Se($4p$)-derived bonding portion of the DOVS for m-Se, from ~3 to ~7 eV, possesses a distinct shoulder on the high-binding-energy side, rather than on the lower-binding-energy side as found for trigonal selenium by UPS.

Our high-resolution DOVS data for t-Se are shown in Fig. 2. They are compared with the data of Shevchik *et al.*,[13] which are shown as a composite spectrum, made up of (high resolution) UPS data from E_F to about 7 eV binding energy, and low-resolution (1.5 eV) XPS data for the Se($4s$)-derived portion of the DOVS from about 8 to 20 eV binding energy. The important features to notice are the slight asymmetry evident in our data in the Se($4p$) nonbinding portion of the data (i.e., from E_F to about 3 eV binding energy) and the equal intensity of the two peak structure in the Se($4p$)-derived bonding portion of the DOVS, from ~3 to ~7 eV binding energy. This latter feature indicates that there are matrix element effects that influence the UPS data for t-Se, in which the electronic final excited states have appreciable conduction-band character and thus differ markedly from the simple plane-wave final states excited in XPS. The Se($4s$)-derived portion of the DOVS's are not significantly different when comparing our data and those of Shevchik *et al.* Note, however, that the monoclinic Se data of Fig. 1 shows a very pronounced dip in the Se($4s$)-derived portion of the DOVS as compared with that of trigonal selenium. We discuss the significance of these differences in the Se($4s$)-derived DOVS's in Sec. IV.

The high-resolution XPS DOVS for o-S is shown in Fig. 3. Note the sharpness of the upper S($3p$)-derived portion of the DOVS, nonbonding for energies from E_F to 4 eV, and bonding for binding energies from 4 to 8 eV. In addition, and perhaps more important, the S($3s$)-derived portion of the DOVS (in the energy range from 8 to 22 eV) is resolved into five distinct features. The energy spacing and relative intensities of these five S($3s$)-derived peaks correspond to the s-mode ring-quantized orbitals,[16,24] i.e., ring modes around an eight-membered ring. The photoemission peaks associated with the individual molecular orbitals were not as well resolved in our earlier studies of S_8 molecules due to the lower resolution of the nonmonochromatic Mg($K\alpha$) radiation employed in that work.[16] Note, however, the significant difference between the S($3s$)-derived (ring mode) portion of the S_8 DOVS and the Se($4s$)-derived (*also* s-electron ring-quantized mode) portion of the Se_8 DOVS. Since the geometry of Se_8 and S_8 are essentially identical, it is evident that such differences in the DOVS must be caused by the alterations in the dynamics of electron motion in

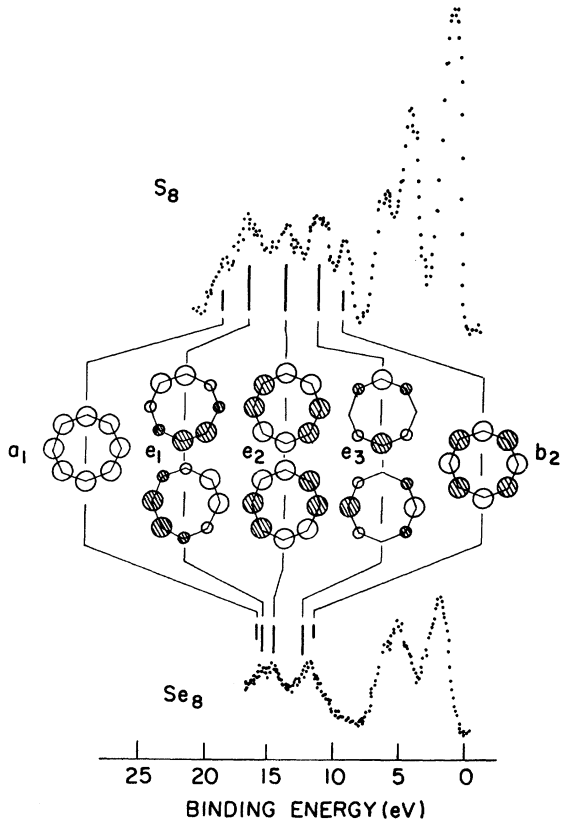

FIG. 3. High-resolution XPS valence-electron photoemission spectra of o-S (top panel) compared with that of m-Se (bottom panel). The s-derived ring-quantized molecular orbitals (Ref. 24) are indicated in the figure, as are their D_{4d} symmetry labels (which contain two corrections to Table II in Ref. 16).

the two materials. In fact, this unusual behavior of the Se 4*s* electrons is caused by the incomplete screening of the Se core by the 3*d* electrons. To see how this effect occurs, however, we must utilize the full CNDO-S formalism.

III. CNDO-S MODEL

Our objective in the analysis of the photoemission spectra described in Sec. II is the construction of a single "spectroscopic" CNDO-S model which describes photoemission and optical absorption data simultaneously.[15-17] To accomplish this end, we previously utilized a standard[25] CNDO model with the off-diagonal matrix elements adjusted in order to describe the UPS photoemission spectra rather than fit to Hartree-Fock results on model systems, as is conventionally done with the common CNDO-2 model.[26] By virtue of this procedure the XPS and ultraviolet absorption spectra have been predictions rather than inputs of our parameterization. For S_8 and S_4N_4 molecules, high-resolution UPS data on the respective molecular vapors were available.[17,27] For Se_8, however, the molecules are unstable and UPS spectra on Se_8 molecules in the vapor are not obtainable in a simple or straightforward way. Thus, we utilize literature values of the various CNDO model parameters rather than selecting the values which best describe gas-phase UPS spectra. The parameter issue is discussed below.

The CNDO model is defined by approximating the Hartree-Fock matrix, constructed in a basis of Slater atomic orbitals, by[26,28]

$$F_{\mu\mu} = U_{\mu\mu} + (P_{AA} - \tfrac{1}{2} P_{\mu\mu})\gamma_{AA} + \sum_{B \neq A} (P_{BB} - Z_B)\gamma_{AB} , \tag{1a}$$

$$F_{\mu\nu} = H_{\mu\nu} - \tfrac{1}{2} P_{\mu\nu}\gamma_{AB} , \quad \mu \neq \nu \tag{1b}$$

if penetration integrals are neglected. The $P_{\mu\nu}$ are the matrix elements of the density matrix (bond-order matrix) in a basis defined by atomic orbitals labeled by μ. The subscripts A and B designate specific atoms in the molecule and indicate summation over all atomic orbitals ϕ_μ on that atom. The γ_{AA} are average single-center Coulomb integrals and γ_{AB} are the corresponding two-center integrals. The $U_{\mu\mu}$ are the one-electron core Hamiltonian matrix elements involving only the ion-core potentials associated with the orbital μ. We use for these quantitites the expression[26]

$$U_{\mu\mu} = I_\mu - (Z_A - 1)\gamma_{AA} , \tag{2}$$

in which I_μ is the ionization potential for the orbital labeled by μ on the atom labeled by A whose net nuclear plus core-electron charge is Z_A.

The off-diagonal matrix elements of the one-electron Hamiltonian are given by the Wolfsberg-Helmholz formula[29]

$$H_{\mu\nu} = \tfrac{1}{2} K(I_\mu + I_\nu)S_{\mu\nu} . \tag{3}$$

The ionization potentials I_μ and intra-atomic Coulomb integrals γ_{AA} are taken from Sichel and Whitehead.[30] The I_{4s} was increased by +1 eV, however, causing a rigid shift of the Se(4s) peaks to appear in better accord with the XPS data. The interatomic two-center Coulomb integrals are obtained using the interpolation formula of Clark[25]

$$\gamma_{AB} = 14.397\{[28.794/(\gamma_{AA} + \gamma_{BB})]^2 + r_{AB}^2\}^{-1/2} , \tag{4}$$

where r is in Å, the parameter 28.794 is in Å/eV and the γ's are in eV. The charge densities in the CNDO-S ground-state calculations were taken to be self-consistent to within one part in 10^3.

The Slater-type atomic orbitals are given by

$$\phi_\mu = A r^{n-1} e^{-\zeta_\mu r} Y_{lm} , \tag{5}$$

where n is the principal quantum number and ζ_μ is the "Slater exponent" for atomic orbital ϕ_μ. Slater originally devised these functions and the ζ_μ to give best fit to SCF atomic energies.[31] In our previous work on chalcogen-containing molecules,[16,17] the ζ_μ were determined by fitting high-resolution gas-phase UPS data. Since that is an intractable task for Se_8, we employ directly essentially the calculated values of ζ_μ as given by Burns.[32]

The CNDO-S calculation produces a self-consistent set of one-electron energy eigenfunctions, which are delocalized molecular orbitals (MO's), corresponding to the Bloch states of an individual molecule. Through Koopman's theorem[33] we expect the one-electron energy spectrum to be a reasonable approximation to the photoemission DOVS, $\rho(E)$. Stated alternatively, we utilize the approximation that relaxation effects are uniform throughout the valence-electron region. The ultraviolet absorption spectra were calculated using

TABLE I. Geometry (Ref. 1) of Se_8.

Atom	x (Å)	y (Å)	z (Å)
1	2.432 723 1	1.007 666 9	0.590 619 5
2	1.007 666 9	2.432 723 1	−0.590 619 5
3	−1.007 666 9	2.432 723 1	0.590 619 5
4	−2.432 723 1	1.007 666 9	−0.590 619 5
5	−2.432 723 1	−1.007 666 9	0.590 619 5
6	−1.007 666 9	−2.432 723 1	−0.590 619 5
7	1.007 666 9	−2.432 723 1	0.590 619 5
8	2.432 723 1	−1.007 666 9	−0.590 619 5

TABLE II. CNDO-S parameters for Se_8 and S_8.

Atom	I_s (eV)	I_p (eV)	I_d (eV)	γ_{AA} (eV)	ζ_s (Å^{-1})	ζ_p (Å^{-1})	ζ_d (Å^{-1})	K_s	$K_p \equiv K_d$
Se	21.8	12.32	2.0	9.12	5.11	3.60	3.60	0.7	0.7
S [a]	20.8	11.98	2.0	9.21	3.21	3.21	2.88	0.5	0.7

[a] Parameters of Ref. 16.

the CNDO-S eigenfunctions as the basis in a configuration-interaction (CI) program based on an analysis like that given by Lowitz.[34] This procedure, which involves no adjustable parameters, permits the construction of electron-hole energy eigenfunctions out of the one-electron energy eigenfunctions. The procedure takes into explicit account the correlation between the electron in an MO above the ground state MO's and the hole in the corresponding ground state MO.

The geometry of Se_8 used in our calculations is specified in Table I. The CNDO-S model parameters are displayed in Table II. The resulting orbital eigenvalues are given in Table III. The low-energy dipole allowed transition states are summarized in Table IV and compared with structure in the imaginary part of the optical dielectric function obtained by Dalrymple and Spear[5] in both Table IV and Fig. 4. Tables I–IV, Fig. 1 and Fig. 4 together specify completely the CNDO-S model and its predictions for Se_8.

TABLE III. CNDO-S eigenvalues for Se_8.

Symmetry (D_{4d})	Energy (eV)
Virtual	
d orbitals	6.8 and above
$1a_2$	−0.58
$4e_1$	−0.64
$4e_2$	−1.08
$4e_3$	−1.81
$3b_2$	−1.83
Occupied	
$3e_3$	−10.42
$3a_1$	−10.56
$3e_2$	−10.97
$3e_1$	−11.52
$2b_2$	−12.87
$2e_1$	−13.63
$1b_1$	−13.75
$2e_2$	−13.90
$2a_1$	−15.15
$2e_3$	−15.37
$1b_2$	−20.79
$1e_3$	−20.70
$1e_2$	−23.83
$1e_1$	−24.93
$1a_1$	−25.23

IV. DISCUSSION

A. Density of valence states (DOVS)

The photoemission spectra of molecules and their corresponding molecular solids are essentially identical, except for some broadening of the spectra in the solid state and a shift of the spectra in the solid state due to a polarization energy.[6] The molecular units within a molecular solid retain their identity as independent entities, interacting only via weak Van der Waals forces. Thus, the predictions of a model of the isolated Se_8 molecule can be directly compared with the spectra of monoclinic selenium, as we already have done with S_8,[16] and S_4N_4.[17]

In particular, the density of valence states ("DOVS"), designated by $\rho(E)$, is constructed from the orbital eigenvalue spectrum (given in Table III) by replacing the eigenvalue of each occupied MO with a Gaussian of 0.75-eV width, to simulate instrumental resolution and solid-state line-broadening effects, then summing over the resulting Gaussians. An illustration of the comparison of the CNDO-S eigenvalue spectrum, the gas-phase UPS valence-electron spectrum[27] and our high-resolution XPS spectrum of o-S is given in Fig. 5. For direct comparison, the high-resolution XPS spectrum of m-Se and the associated CNDO-S eigenvalue spectrum also are shown in this figure.

Some of the general features of the XPS valence-electron spectrum can be understood, however, without appeal to the details of the CNDO-S model. As as immediate consequence of the large dif-

TABLE IV. Comparison of measured peaks in $\mathrm{Im}\epsilon(\omega)$ of monoclinic selenium [a] with the CNDO-S transition-state eigenvalues obtained using a 7×5 configuration-interaction analysis.

Peaks in $\mathrm{Im}\epsilon(\omega)$ [a] (eV)	Allowed transitions CNDO-S (CI) (eV)	Symmetry
3.2	3.6	B_2
4.2	3.8	E_1
$\sim 5\frac{1}{2}$	5.5 5.6 5.7	E_1 E_1 B_2
6.4	6.5	B_2, E_1

[a] Dalrymple and Spear, Ref. 5.

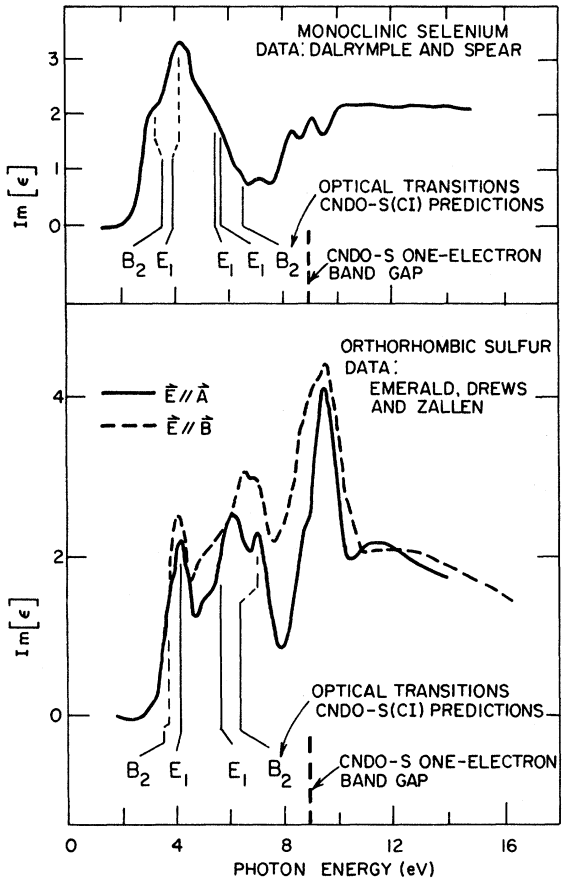

FIG. 4. Comparison of the imaginary part of the optical dielectric function for α-m-Se reported by Dalrymple and Spear (Ref. 5) with dipole-allowed CNDO-S transition energies. Analogous results for o-S also are reproduced from Ref. 16.

ference between the Se(4s) ionization potential ($I_s = 21.8$ eV) and the Se(4p) ionization potential ($I_p = 12.32$ eV), the DOVS in the energy range $E_B \leq 8$ eV correspond to Se(4p)-derived states, while for $8 \leq E_B \leq 20$ eV the DOVS correspond to Se(4s)-derived states. The same is true for sulfur, which has $I_p = 11.98$ eV and $I_s = 20.77$ eV. In the case of S_8, the photoemission from the S(3s)-derived states is described qualitatively by a simple tight-binding model, i.e.,[12,35]

$$E_s(m) = I_s - 2V_{s1}\cos(\tfrac{1}{4}\pi m) - 2V_{s2}\cos(\tfrac{1}{2}\pi m)\,, \quad (6)$$

in which V_{s1} is the nearest-neighbor interaction and $V_{s2} \simeq 0$ is the next-nearest-neighbor interaction. The $m = 0$ eigenvalue corresponds to the $1a_1$ orbital in Table III, with the $m = 1, 2, 3$ eigenvalues corresponding to the $1e_m$ orbitals and the $m = 4$ eigenvalue to the $1b_2$ orbital, respectively.[24] In Se_8, however, this simple ring-quantized orbital pattern with degeneracies 1-2-2-2-1 is spoiled by Coulomb correlations: a topic to which we shall return later. The s-derived orbital identifications for the XPS spectra of S_8 and Se_8 are illustrated pictorially in Fig. 3.

In contrast to the photoemission from the atomic s-derived states, the DOVS corresponding to the p-derived states of m-Se and o-S are nearly identical: a result illustrated clearly in Fig. 5. The similarity of the CNDO-S p-derived orbital eigenvalue spectra in S_8 and Se_8 molecules also is evident from Fig. 5. This result could have been anticipated from inspection of Table II from which we see that the K_p value is the same in the two cases; the p-electron ionization potentials for S and Se are nearly identical[30]; and the Slater rules[32] produce a ζ_p for Se which is almost equal to the value obtained in Ref. 16 for S_8 by fitting the gas-phase UPS spectra.[27]

Figure 5 reveals that the p-derived XPS DOVS for both m-Se and o-S exhibits a three-peak

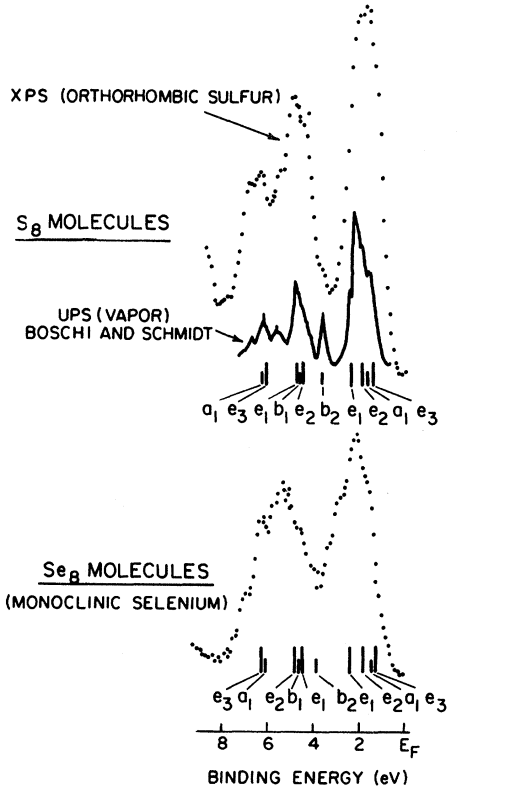

FIG. 5. Comparison of the p-derived portion of our high-resolution XPS valence-electron photoemission spectrum of o-S with the UPS spectra (Ref. 27) of gas-phase S_8 (upper two curves). The p-derived portion of the m-Se XPS valence-electron spectrum also is shown for comparison with that of o-S, as are the p-derived CNDO-S eigenvalue spectra of S_8 and Se_8, respectively. The labeling of the eigenvalue spectra for S_8 shown in the figure contains one correction to the version given in Table II and Fig. 4 of Ref. 16.

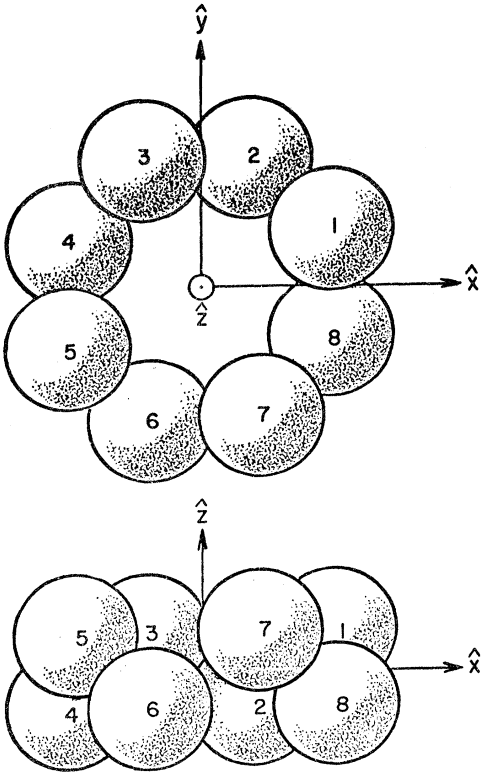

FIG. 6. Schematic indication of the coordinate system utilized to describe S_8 and Se_8.

structure, with a large peak at small binding energies, $E_B \lesssim 3$ eV, and a broader maximum in the vicinity of $4 \lesssim E_B \lesssim 8$ eV which is split into two components. Moreover, from Fig. 2 it is clear that this same general pattern persists in t-Se, although the intensity distribution in the higher-binding-energy doublet is altered slightly. In the case of trigonal Se, the low-binding-energy maximum has been attributed to "lone-pair" electrons in p orbitals oriented normal to the local-coordination plane determined by a given Se atom and its two nearest neighbors.[8-10] In this "empirical pseudopotential model" (EPM) the higher-binding-energy split peak is associated with "bonding" p-derived orbitals which lie in the local-coordination plane.

Because of the plausibility and simplicity of this EPM model for p-electron photoemission from p-derived orbitals, as well as its presumed broad applicability to all solids comprised of elements from column VI of the Periodic Table,[20] we examined our CNDO-S eigenvalues for S_8 and Se_8 to verify their consistency with it. We found, quite to our initial surprise, that whereas the molecular orbitals contributing to the lower-binding-energy peak are less bonding than those in the higher-binding-energy peak in the traditional chemical sense,[36] they are not comprised of the linear combinations of S and Se atomic orbitals envisaged in the EPM. Utilizing the coordinate system shown in Fig. 6, we may classify the symmetry-adapted p-derived orbitals[24,37] for the D_{4d} molecular symmetry as π orbitals normal to the x-y plane, and radial and tangential orbitals within the x-y plane. These symmetry adapted orbitals are either bonding (a_1—radial, b_2—π, b_1—tangential, e_1—radial, e_3—π and tangential), nonbonding (e_2), or antibonding (b_2—radial, a_1—π, a_2—tangential, e_3—radial, e_1—tangential and π) in character, and the CNDO-S eigenstates consist of linear combinations thereof. Thus, from the traditional chemical perspective,[24,35,37] the low-binding-energy peak, $E_B \lesssim 3$ eV (see Fig. 5) is comprised of a mixture of one e_2 nonbonding radial-tangential hybrid, one (a_1) antibonding π orbital, and two (e_1, e_3) hybrids between antibonding π orbitals and bonding radial-tangential orbitals. The center p-derived emission peak $8 \gtrsim E_B \gtrsim 4$ eV contains the nonbonding π orbital (e_2), the bonding tangential orbital (b_1) and other hybrid bonding orbitals. The highest-binding-energy p-derived emission peak contains the bonding radial orbital (a_1) and a heavily hydridized bonding π orbital (e_3).

Because of the symmetry of the S_8 and Se_8 molecules, the symmetry-adapted basis functions and the CNDO-S eigenfunctions are constructed from linear combinations of atomic orbitals which exhibit either p_z (i.e., π), radial, or tangential character relative to the x-y plane of the molecule. Consequently, they are not simply related to the EPM "bonding p" and "lone-pair" atomic orbitals which are defined relative to the local planes specified by three nearest-neighbor S or Se atoms.[8-11,20] In particular, the radial and π symmetry-adapted basis functions consist of comparable admixtures of EPM "lone-pair" and "hybridized-p-like" basis functions. Therefore irrespective of the properties of charge density averaged over a prescribed energy interval, the CNDO-S eigenstates of Se_8 do not correspond to those predicted by the EPM.

The symmetry-adapted-orbital approach also may be used[38] to interpret the differences in the p-electron emission spectra of m-Se and t-Se. The above analysis reveals that in the D_{4d} geometry, the p-derived orbital eigenvalues cluster in a 3:5:7 pattern in order of decreasing binding energy. In a six-atom C_{2v} geometry [i.e., hypothetical (boat geometry)] the cluster pattern is[24] 3:4:5. Both results yield the middle p-electron emission peak to be more intense than the highest-binding-energy peak as observed in m-Se, o-S,

and amorphous Se.[13] In t-Se, on the other hand, use of a planar Se_3 molecular cluster for each unit cell along the Se chains immediately predicts a 2 : 1 : 3 pattern,[38] in precise accord with the observed alterations in line shape, displayed in Figs. 1 and 2, incurred when comparing m-Se with t-Se.

We conclude this subsection with a consideration of the differences in the s-derived photoemission spectra of o-S and m-Se. We already have noted in conjunction with Eq. (6) that the s emission is described qualitatively by a Hückel nearest-neighbor-interaction model of ring-quantized $S(3s)$ orbitals. In m-Se, however, a roughly 1:1 doublet s emission is observed in contrast to the 1:2:2:2:1 pattern characteristic of o-S. The reason for this difference may be discerned from Table II and Eq. (1b). The imperfect screening of the Se core by its $3d$ electrons result in the large Slater exponent for the Se($4s$) orbital given in Table II.[32] This large exponent, in turn, reduces the next-nearest-neighbor interaction in the $H_{\mu\nu}$ term in Eq. (1b) to the point that the off-diagonal Fock operator, $F_{\mu,\mu+2}$, is dominated by the Coulomb correlation contribution, $-\frac{1}{2}P_{\mu,\mu+2}\gamma_{\mu,\mu+2}$. This term is large and attractive for the nonbonding ($1e_2$) s-electron ring-quantized orbital, thereby depressing this orbital to near degeneracy with the $1e_1$ orbital (for which the next-nearest-neighbor Coulomb correlations tend to average out). This effect, together with the generally smaller value of $H_{\mu,\mu+1}$ caused by the large value of ξ_{4s} for Se, collapse the 1 : 2 : 2 : 2 : 1 tight-binding pattern into a 5 : 3 Coulomb-correlation-driven pattern. The corresponding phenomenon is less severe but still substantial in the planar Se_3 cluster used to model t-Se, tending to create to a 1 : 2 pattern rather than a 1 : 1 : 1 pattern.[38] Therefore we expect to find a doublet s-derived photoemission pattern in *both* m-Se and t-Se, in accord with the spectra shown in Figs. 1 and 2. The failure of existing Hückel calculations[19] to describe quantitatively either the s-derived or the p-derived photoemission from m-Se also is displayed explicitly in Fig. 1.

B. Ultraviolet absorption spectrum (UVA)

As in the case of the DOVS, the ultraviolet absorption (UVA) of a molecular solid can be analyzed in terms of that of its constituent molecules. In the absence of polarization measurements, this procedure is equivalent to an application of the oriented gas model[39] in which the factor-group (Davydov) splittings are neglected.

Comparisons of the predicted energies of the CNDO-S (CI) allowed transition states of Se_8 and S_8 with the imaginary part of the optical dielectric function [i.e., $\epsilon_2(h\nu)$] for m-Se and o-S are displayed in Fig. 4, where 7 occupied and 5 unoccupied states were used in the initial manifold for the CI computation. It is evident that the major structure in $\epsilon_2(h\nu)$ for $2 \lesssim h\nu \lesssim 4$ eV can be identified with molecular excitons, since the one-electron band gap (see Table III) is almost 9 eV. Moreover, this result is entirely consistent with the known photogeneration of carriers from these optically excited states because the strong intermolecular electronic polarization created by the resulting isolated electrons and holes renders even tightly bound molecular excitons unstable against dissolution into electron-hole pairs.[40] Thus, we interpret the low-energy, $2 \lesssim h\nu \lesssim 4$ eV, UVA in m-Se and o-S in terms of molecular excitons rather than interband transitions[5,7,18]: an interpretation constant with that of the DOVS given in the preceeding subsection.

The only measurement which is not predicted clearly by our CNDO-S (CI) analysis of singlet optically excited states is the 2.55-eV low-temperature absorption line reported by Knights and Davis.[18] The major edge of the observed m-Se UVA occurs just below $h\nu = 3$eV, however, and our CNDO-S (CI) analysis predicts a single-triplet transition state 0.4 eV below the lowest-energy singlet state. Therefore we believe that the 2.55-eV line is a triplet exciton absorption which is observable because of large spin-orbit coupling associated with the poor screening of Se core by the Se($3d$) electrons. Since Se_8 does not exist in the vapor, confirmation of molecular as opposed to interband nature of the 2.55-eV absorption line will have to emerge its observation either for Se_8 in solution or of Se_8 absorbed on a surface. An observation of the same UVA spectrum for isolated Se_8 molecules as for m-Se would prove the molecular nature of m-Se and negate any interband transition models for the optical spectrum of m-Se. Definitive assessment of its triplet nature may be more difficult, however, because we cannot rule out with certainty its being the zero-vibaration $^1B_2$ exciton line, lowered in energy relative to molecular Se_8 by its intermolecular electronic polarization self-energy.[40]

V. SUMMARY

In Figs. 1–3 the first measurements of high-resolution XPS valence-electron emission spectra for m-Se, t-Se, and o-S are presented. These spectra reveal structure in the photoemission DOVS from p-derived molecular orbitals (small binding energy $E_B \lesssim 8$ eV) comparable to that observed by UPS measurements,[13] thereby suggesting that solid-state effects rather than instrumental resolution constitute the limitation on the

sharpness of such spectra.

To interpret the data shown in Figs. 1–3 we evaluated the CNDO-S orbital eigenvalue spectrum of Se_8. Figure 1 reveals that the density of valence states obtained from these eigenvalues provides a quantitative description of the XPS measurements. Moreover, we see from Fig. 4 that a configuration-interaction analysis of transition states obtained from the CNDO-S eigenfunctions provides a semiquantitative description of optical absorption[5] ($2 \leq h\nu \gtrsim 4$ eV) in m-Se in terms of molecular excitons. Since both results are comparable to those obtained in our earlier study[16] of o-S, we conclude that the electronic structures of the Van der Waals solids m-Se and o-S are dominated by those of their constituent molecules, Se_8 and S_8, respectively, i.e., they are true Van der Waals solids.

The availability of CNDO-S models for a number of molecular chalcogenides[15-17] further permitted us to perform a systematic study of the relationship between molecular geometry and electronic structure.[24] As summarized in Sec. IV A, in the case of the Se_8 and S_8 molecules (i.e., D_{4d} symmetry) each maximum in the XPS valence-electron spectra can be associated with a group of symmetry-related one-electron orbitals. These patterns are almost identical for p-derived photoemission from S_8 and Se_8, although the poor screening of the nuclear charge by the Se(3d) electrons creates Coulomb correlations which severely distort the s-derived photoemission patterns for m-Se and t-Se. All differences in the emission spectra from t-Se relative to m-Se can be understood, however, on the basis of the altered symmetry of the (planar) three-atom unit cell in t-Se relative to puckered Se_8 rings.[38] We believe, therefore, that our general symmetry arguments as supplemented by the detailed dynamics of the CNDO-S model afford a precise interpretation of all major structure observed in both the XPS and UVA spectra of the molecular chalcogens o-S and m-Se.

And finally, in comparing the Se(4s)-derived portion of the XPS DOVS of t-Se with that of amorphous (a-) Se, other authors[10] have argued against the existence of eight-membered rings in a-Se, which consists of a mixture of rings and chains.[41] The "dip" in the Se(4s)-derived portion of the XPS DOVS for a-Se is slightly deeper than that for t-Se. A tight-binding model (either EPM or Hückel) would predict the tight-binding sequence of ring-quantized orbitals as seen in sulfur. Both the experiment *and* our CNDO-S model reveal, however, that Se_8 rings result in a distinct "dip" in the Se(4s)-derived structure in the XPS DOVS. Thus, the XPS DOVS data on t-Se, m-Se, and a-Se are consistent with the presence of Se_8 rings in a-Se, rather than evidence against it.

ACKNOWLEDGMENTS

The authors are indebted to G. Lucovsky and J. Knights for a critique of the evidence for molecular bonding in m-Se; to K. L. Yip for communicating results to us prior to publication; to K. S. Liang, J. W-p. Lin, P. Nielsen, and L. B. Schein for helpful discussions; to D. Roll and R. Geils for assistance in preparing samples; and to L. Kennedy for assistance.

[1]P. Unger and P. Cherin, in *Physics of Selenium and Tellurium*, edited by W. C. Cooper (Pergamon, Oxford, 1969), p. 223.
[2]W. C. Cooper and R. A. Westbury, in *Selenium*, edited by R. A. Zingaro and W. C. Cooper (Reinhold, New York, 1974), p. 87.
[3]S. C. Abrahams, Acta. Crystallogr. 8, 661 (1955).
[4]A. Caron and J. Donohue, Acta. Crystallogr. 14, 548 (1961).
[5]R. J. F. Dalrymple and W. E. Spear, J. Phys. Chem. Solids 33, 1071 (1972).
[6]C. B. Duke, W. R. Salaneck, A. Paton, K. S. Liang, N. O. Lipari, and R. Zallen, in *Proceedings of the International Conference on Structure and Excitations of Amorphous Solids*, edited by G. Lucovsky and F. L. Galeener (AIP, New York, 1976); Bull. Am. Phys. Soc. 21, 458 (1976).
[7]J. Stuke, in *Selenium*, edited by R. A. Zingaro and W. C. Cooper (Van Nostrand Reinholt, New York, 1974), p. 174.
[8]M. Schlüter, J. D. Joannopoulos, and M. L. Cohen, Phys. Rev. Lett. 33, 89 (1974).
[9]N. J. Shevchik, Phys. Rev. Lett. 33, 1572 (1974).
[10]J. D. Joannopoulos, M. Schlüter, and M. L. Cohen, Phys. Rev. B 11, 2186 (1975).
[11]D. W. Bullett, J. Phys. C 8, L377 (1975).
[12]J. Robertson, J. Phys. C 8, 3131 (1975).
[13]N. J. Shevchik, M. Cardona, and J. Tejeda, Phys. Rev. B 8, 2833 (1973).
[14]M. Kastner and R. R. Forberg, Phys. Rev. Lett. 36, 740 (1976).
[15]W. R. Salaneck, K. S. Liang, A. Paton, and N. O. Lipari, Phys. Rev. B 12, 725 (1975).
[16]W. R. Salaneck, N. O. Lipari, A. Paton, R. Zallen, and K. S. Liang, Phys. Rev. B 12, 1493 (1975).
[17]W. R. Salaneck, J. W-p. Lin, A. Paton, C. B. Duke, and G. P. Ceasar, Phys. Rev. B 13, 4517 (1976).
[18]J. C. Knights and E. A. Davis, Solid State Commun. 11, 543 (1972).
[19]I. Chen. Phys. Rev. B 11, 3976 (1975); B 7, 3672 (1973).
[20]M. Kastner, Phys. Rev. Lett. 28, 355 (1972).
[21]K. Siegbahn, J. Electron. Spectros. Relat. Phenom. 5, 3 (1974).
[22]A. Barrie (unpublished).
[23]C. H. Griffiths and H. Sang, Appl. Phys. Lett. 11, 118

(1967).
[24]C. B. Duke and W. R. Salaneck, Bull. Am. Phys. Soc. 21, 228 (1976); and unpublished.
[25]D. T. Clark, Tetrahedron 24, 2663 (1968).
[26]J. A. Pople and D. L. Beveridge, *Approximate Molecular Orbital Theory* (McGraw-Hill, New York, 1970).
[27]R. Boschi and W. Schmidt, Inorg. Nucl. Chem. Lett. 9, 643 (1973).
[28]N. O. Lipari and C. B. Duke, J. Chem. Phys. 63, 1748 (1975); 63, 1767 (1975).
[29]M. Wolfsberg and L. Helmholz, J. Chem. Phys. 20, 837 (1952).
[30]J. M. Sichel and M. A. Whitehead, Theor. Chim. Acta 7, 32 (1967).
[31]J. C. Slater, Phys. Rev. 36, 57 (1930).
[32]G. Burns, J. Chem. Phys. 41, 1521 (1964).
[33]T. Koopmans, Physics 1, 104 (1933).
[34]D. A. Lowitz, J. Chem. Phys. 46, 4698 (1967).
[35]J. D. Joannopoulos and M. L. Cohen, Phys. Rev. B 7, 2644 (1973).
[36]L. Salem, *The Molecular Orbital Theory of Conjugated Systems* (Benjamin, New York, 1972), Chaps. 1 and 7.
[37]F. A. Cotton, *Chemical Applications of Group Theory*, 2nd ed. (Wiley, New York, 1971), Chaps. 6 and 7.
[38]C. B. Duke and K. L. Yip (unpublished).
[39]D. P.Craig and S. H. Walmsley, *Excitons in Molecular Crystals* (Benjamin, New York, 1968), Chap. 3.
[40]C. B. Duke, University of Rochester Lecture notes, 1975 (unpublished).
[41]G. Lucovsky, A. Mooradian, W. Taylor, G. B. Wright, and R. C. Keezer, Solid State Commun. 5, 113 (1967); an excellent recent review is R. Zallen and G. Lucovsky, in *Selenium*, edited by R. A. Zingaro and W. C. Cooper (Reinhold, New York, 1975), Chap. 5.